Nonlinear Phenomena in Complex Systems, vol. **13**, no. 1 (2010), pp. 70 - 78

Cautionary Example of Nonlinear Time Series Analysis: From Tones to Sounds

Said Bešlagić and Matjaž Perc*
Department of Physics, Faculty of Natural Sciences and Mathematics, University of Maribor, Koroška cesta 160, SI-2000 Maribor, SLOVENIA
(Received 23 September, 2009)

We study the route from basic tones towards sounds and chords in terms of dynamical complexity of the underlying time series of the sound recordings. Although this route offers increasingly complex waveforms for the analysis, we provide conclusive evidences that even the most complex of them is still periodic. The employed methods of nonlinear time series analysis leading to this conclusion are very instructive, showing how to avoid pitfalls and false claims when trying to distinguish experimentally obtained chaotic traces from those that merely incorporate a large number of harmonic and inharmonic frequencies yet are still periodic. We use methods of nonlinear time series analysis as well as waveforms outputted by a frequency generator and actual recordings of picked guitar strings for the analysis, thus employing resources that are readily available in the lab as well as classrooms.

PACS numbers: 05.45.Tp, 05.45.Ac
Keywords: quasiperiodicity, chaos, times series analysis, stringed instruments

1. Introduction

Ever since the discovery of deterministic chaos in nonlinear dynamical systems the subject has been very popular [1–4], receiving continuous attention from the scientific as well as general audience. Not surprisingly, the lure of chaos has been used rightfully to captivate and inspire students for the subject of nonlinear dynamics already at an early stage of the educational process. In particular, several computer simulations and simple experiments have been proposed to accomplish this task [5–8]. While simulations are often very clear and instructive, experiments arguably posses the ability to leave a more profound impact on the audience due to their better connectedness to real life and with it related vivid experience of the phenomenon. However, the experimental approach also brings along certain difficulties that are sometimes hard to overcome in graduate and undergraduate courses. Specific problems are related to the acquisition of data from the experimental setting and to the subsequent analysis of the resulting time series. While former are experiment specific and usually require special equipment in order to be surpassed, the latter can be effectively tamed with methods of nonlinear time series analysis [9–11].

Presently, we wish to elaborate on the pitfalls and difficulties associated with the time series analysis of experimental traces, specifically by showing that complex temporal outlays visually lacking a repeating pattern of activity, and phase space plots with no closed paths of the trajectory, may still be insufficient to demonstrate chaotic behavior in the classroom. In particular, we warn from using sophisticated methods of nonlinear time series analysis on such traces, as they might lead to an indication of chaos solely due to the complexity of the employed method rather than the inherent complexity in the studied time series. Thus, the following text introduces a critical point of view on the employment of certain techniques, and perhaps more importantly, shows how simple methods may be superior in correctly characterizing the behavior in accordance with the actual physics behind it.

To accomplish the designated goal, we study the transition from isolated tones, generated by a frequency generator, towards sounds and

*E-mail: matjaz.perc@uni-mb.si

chords of a guitar. While an isolated tone is characterized by a single sound frequency, *e.g.* 110.0Hz, without higher harmonics, and thus its waveform corresponds to a simple sinusoidal curve, the sound of the corresponding guitar string is a conglomerate of the ground frequency 110.0Hz plus its higher harmonics, *i.e.* modes, resulting in a more complex yet still periodic wave form [12]. A guitar of reasonable quality produces at least five higher harmonics of the ground frequency of the string, while guitars of exceptional quality yield up to ten, giving the sound a warm and well-balanced sensation. An even more complex waveform can be obtained by playing several strings simultaneously to yield a guitar chord, which besides the ground frequency and its (almost) higher harmonics, is supplemented by additional tones that are not higher harmonics of the ground frequency. For example, chord A with the ground frequency of 110.0Hz is obtained by simultaneously playing also strings Cis and E with ground frequencies of 138.6Hz and 164.8Hz, respectively. These accompanying tones give the chord additional richness and contribute to the harmony of the sound. More importantly, however, due to the vast number of excited harmonic and inharmonic (note the ratio between the ground frequencies of Cis, E, and A) modes of each individual string as well as the body of the instrument, the resulting waveform of a guitar chord is very complex, lacking an obvious repeating pattern upon visual inspection. Moreover, the reconstruction of the phase space, as described in the next section, yields a plot similar to those obtained when studying deterministic chaotic systems. Thus, without an in-dept knowledge of the physics behind the mechanics of vibrating strings [13] it is quite inviting to conclude that one is observing a deterministic chaotic system. By employing methods of nonlinear time series analysis, we will show that in fact such an assessment is wrong, and that in spite of the vast number of harmonic and inharmonic frequencies incorporated in such traces, the behavior is still periodic. In sum, we will study the transition from tones of a frequency generator towards sounds of an isolated and multiple guitar strings to show that, despite of the apparent increase of the complexity in the resulting waveforms, even the most complex one is still an example of periodic behavior.

Finally, we also provide user-friendly programs with graphical interface for each implemented method [14], which should make the reproduction of presented results possible even for individuals with little or no experience with the presented theory, and also facilitate further applications on other experimental recordings. An extremely versatile collection of programs for the time series analysis is also available through the TISEAN project [15, 16]. We recommend greatly to exploit the benefits offered by theses sources.

2. Results

In order to obtain the waveforms, the frequency generator was plugged into a speaker and the resulting sound was recorded via the sound card of a personal computer. Sounds of guitar strings were recorded directly, *i.e.* without the additional speaker support. Each sound was sampled at 44kHz ($dt = 2.27 \cdot 10^{-5}$). Since we focus on sounds with the ground frequency of 110.0Hz, corresponding to the A note, up to two seconds long recordings suffice to capture the relevant dynamics of the resulting waveforms. Prior to the examination with methods of nonlinear time series analysis, all waveforms were re-scaled in amplitude to the unit interval to enable a better comparison of obtained results.

We start by examining the waveform of a frequency generator at 110.0Hz. Note that frequency generators yield sounds that are characterized by a single frequency. In other words, no higher harmonics are produced. Accordingly, the sound produced by a frequency generator appears dull, resembling a monotonous humming, and its waveform is nothing more than a sinusoidal curve, as presented in the left panel of Fig. 1(a). In the terminology of dynamical systems such a temporal output would be considered as a simple periodic solution,

which can be obtained by solving for example the well-know harmonic oscillator $\ddot{x} + \omega x^2 = 0$ (although the physics behind the harmonic oscillator has little in common with the physics of vibrating strings or the output of a frequency generator, we mention this example here to give an intuitive and convenient explanation of the embedding theorem and the result obtained via Eq. 2 latter in the text). The phase space of such a solution corresponds to a limit cycle attractor. In order to visualize the limit cycle without the use of mathematical models we have to reconstruct the phase space from the waveform of the sound recording. For this purpose the embedding theorem [17] must be employed, which states that for a large enough embedding dimension m, the delay vectors

$$\mathbf{p}(i) = [x_i, x_{i+\tau}, x_{i+2\tau}, \ldots, x_{i+(m-1)\tau}] \quad (1)$$

yield a phase space that has exactly the same properties as the one formed by the original variables of the system (*e.g.* the two variables of the harmonic oscillator). In Eq. 1 variables $x_i, x_{i+\tau}, x_{i+2\tau}, \ldots, x_{i+(m-1)\tau}$ denote values of the waveform, as the one presented in Fig. 1(a), at times $t = idt, t = (i + \tau)dt, t = (i + 2\tau)dt, \ldots, t = [i + (m-1)\tau]dt$ respectively, where τ is the so-called embedding delay. Although the implementation of Eq. 1 is straightforward, we first have to determine proper values of m and τ. However, since currently we want only to visualize the phase space in a two-dimensional graph, we restrict ourselves to determining a proper embedding delay τ, thus obtaining the two necessary variables x_i and $x_{i+\tau}$.

If the temporal trace is not particularly irregular, a suitable τ can be estimated from the autocorrelation function

$$a(\Delta) = \frac{1}{n}\sum_{i=1}^{n} x_i x_{i+\Delta}, \quad (2)$$

in particular, by the time delay Δ the autocorrelation function drops to zero. For the waveform presented in Fig. 1(a) this procedure yields $\tau = 100$. The corresponding phase space is presented in the right panel of Fig. 1(a). Indeed, it can be observed nicely that a simple limit cycle attractor is obtained that is identical to the one we can observe by solving the harmonic oscillator if ω and the initial displacement are both equal to 1. Interestingly, note that $\tau = 100$ corresponds exactly to 1/4 of the oscillation period of the signal with the frequency 110.0Hz if sampled at 44kHz. Put otherwise, if the oscillation period would be 2π, as by the harmonic oscillator, the procedure would yield $\tau = \pi/2$. Finally, since the displacement by the harmonic oscillator obeys $x(t) = cos(t)$ and the velocity $\dot{x}(t) = y(t) = sin(t)$ (provided the initial displacement and ω are equal to 1), note that indeed $y(t) = x(t - \tau)$, which can be seen as a simple justification of Eq. 1. Note that Eq. 1 can be formulated identically with delay components $x_i, x_{i-\tau}, x_{i-2\tau}, \ldots, x_{i-(m-1)\tau}$.

Before we proceed by analyzing sounds of isolated and multiple guitar strings, we will use the frequency generator once more in order to make the transition to complex sounds smoother. Recall from the Introduction that a sound from an isolated guitar string may incorporate up to ten higher harmonics of the ground frequency. Thus, in order to mimic this we record also two higher harmonics of the A note (110.0Hz) with the frequency generator and merge these into two new waveforms, one comprising the frequencies 110.0Hz+220.0Hz and the other the frequencies 110.0Hz+220.0Hz+330.0Hz, respectively. By listening to the resulting sounds, one can easily identify the increase of sound richness and complexity as the number of higher harmonics increases. In accordance with this perception the complexity of the underlying waveforms also increases, as can be observed by comparing temporal traces and the pertaining phase spaces in Figs. 1(a) to (c). The embedding delays for phase spaces in Figs. 1(b) and (c) equal $\tau = 50$ and $\tau = 33$, respectively, and were obtained with the same procedure as was used for the phase space presented in Fig. 1(a).

In order to further continue in the spirit of the above-outlined increase of complexity in the studied sound recording, we now turn to studying sounds of isolated and multiple guitar strings.

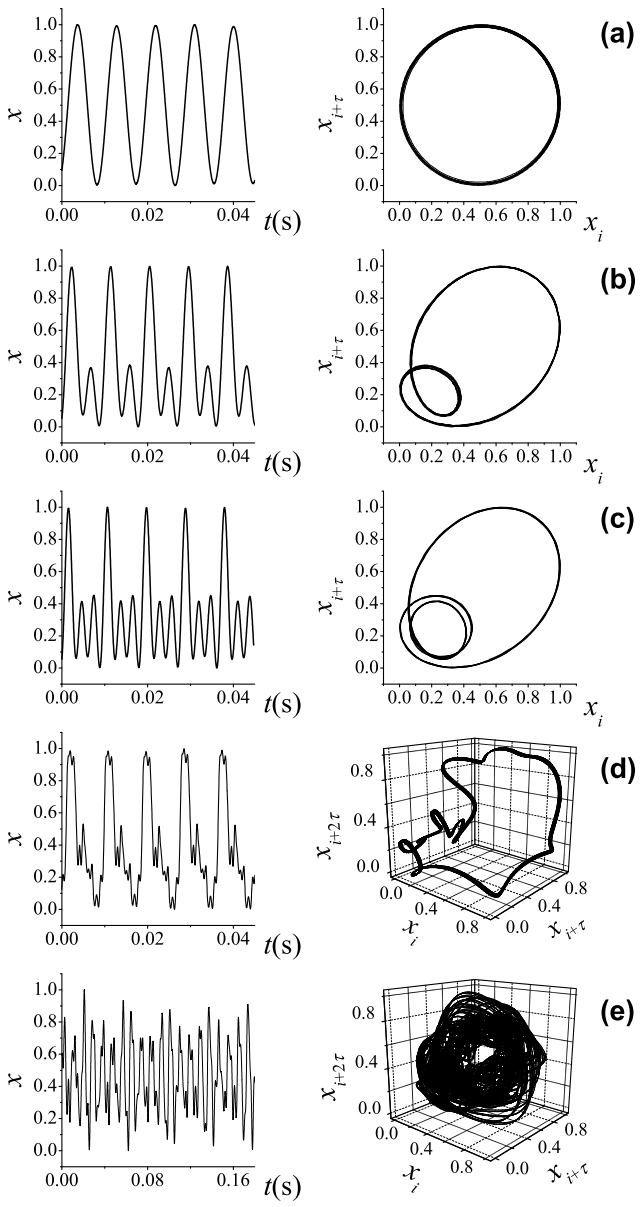

FIG. 1. Temporal traces and pertaining phase space reconstructions for different sounds increasing in complexity from top to bottom. The last two phase space portraits are shown as three-dimensional graphs in order to better reveal the complexity of the underlying attractors. Also, the time span for the bottom temporal trace is four times larger than in the upper panels to better convey the irregularity of the series.

Naturally, the string of our choice is string A (second from the top on a six string guitar) as it has the same ground frequency as our previous recordings. The resemblance of the sound of the guitar string with that of the frequency generator comprising the three harmonics [Fig. 1(c)] is quite remarkable, although the quality and richness of the latter is obviously inferior. Indeed, the waveform of the guitar string shown in the left panel of Fig. 1(d) is more complex than the one in Fig. 1(c). Still, however, the ground frequency and the periodicity in the temporal trace are expressed nicely. Due to the substantial complexity of the waveform in Fig. 1(d), however, the proper embedding delay τ can no longer be faithfully determined by the autocorrelation function $a(\Delta)$ given by Eq. 2, because the latter does not take into account possible nonlinear correlations between distinct points of the time series. In order to surpass this problem, we must calculate the mutual information in dependence on the delay Δ. The mutual information $I(\Delta)$ between x_i and $x_{i+\Delta}$ quantifies the amount of information we have about the state $x_{i+\Delta}$ presuming we know the state x_i [18]. Given a time series, one first has to find the minimum (x_{min}) and the maximum (x_{max}) of the sequence. The absolute value of their difference $|x_{max} - x_{min}|$ then has to be partitioned into j equally sized intervals, where j is a large enough integer number. Finally, one calculates the expression

$$I(\Delta) = -\sum_{h=1}^{j}\sum_{k=1}^{j} P_{h,k}(\Delta)\ln\frac{P_{h,k}(\Delta)}{P_h P_k}, \qquad (3)$$

where P_h and P_k denote the probabilities that the variable assumes a value inside the h-th and k-th bin, respectively, and $P_{h,k}(\Delta)$ is the joint probability that x_i is in bin h and $x_{i+\Delta}$ is in bin k. Fraser and Swinney [19] argued that the first minimum of $I(\Delta)$ is a suitable candidate for the optimal embedding delay τ. Applying Eq. 3 on the waveform presented in Fig. 1(d) yields $\tau = 30$. The pertaining phase space in three dimensions is shown in the right panel of Fig. 1(d). Note that we have switched to the three-dimensional view in order to better reveal the complexity of the underlying limit cycle. Depending on the projection angle the limit cycle in Fig. 1(d) is folded at least five times, thus

exceeding the complexity of its predecessor in Fig. 1(c) substantially. Again, however, we can conclude without a doubt that the resulting trace is an example of complex, yet fully periodic behavior as the cycles repeat seamlessly in the phase space.

Finally, it remains of interest to examine the most complex sound within this study, namely the waveform of a guitar chord A, which as foretold in the preceding section, will pose a puzzle with regard to the determination of the type of behavior it represents (chaotic or periodic). As already mentioned in the Introduction, the chord A is obtained by simultaneously playing string A with the ground frequency of 110.0Hz as well as strings Cis and E with ground frequencies of 138.6Hz and 164.8Hz, respectively. The two accompanying tones give the chord additional richness in comparison to the sound of an isolated A string, thus contributing to the harmony of the sound. This can be verified easily by listening to the sound of a guitar chord and comparing it to the sound of a single plucked string. The increased complexity of the sound can be identified visually by inspecting the pertaining waveform that is presented in the left panel of Fig. 1(e). Indeed, while the predominant ground frequency of 110.0Hz can still be inferred quite well from the waveform, the regular periodicity that can be identified in upper temporal traces is apparently no longer at hand. The irregularity of the temporal trace is vividly reflected also in the reconstructed phase space that is shown in the right panel of Fig. 1(e). The embedding delay for the phase space in Fig. 1(e) equals $\tau = 70$ and was obtained via Eq. 3 as for Fig. 1(d). By acknowledging the fact that each guitar string yields up to ten harmonics (see also footnote in [12]) in the resulting waveform, as can be inferred from Fig. 1(d), plus the fact that the simultaneous action of multiple strings that have irrational relations of their ground frequencies yields a non-closed trajectory in the phase space, it is easy to trace back the resulting complexity in the guitar chord.

In view of this complexity assessed via visual inspection of Fig. 1(e), one may be tempted to declare chaos in the presented temporal trace. However, in order to confirm this conclusively, we need to calculate the maximal Lyapunov exponent Λ_{max} of the series. If the latter is positive, this can be considered a proof of the fact that the studied sound recording originated from a chaotic system. On the other hand, $\Lambda_{max} = 0$ is characteristic for periodic solutions, as shown in the upper panels of Fig. 1. In order to successfully calculate Λ_{max} from the temporal trace we still have to determine the dimensionality (embedding dimension) m of the underlying system. In other words, we must determine the number of active degrees of freedom the attractor needs to fully evolve in the phase space, or equivalently, how many autonomous first order ordinary differential equations we need in order to mathematically model the studied behavior. In order to do so we employ the so-called false nearest neighbor method that was presented by Kennel *et al.* in [20]. The method relies on the assumption that points that are close in the reconstructed phase space have to stay sufficiently close also during forward iteration. If this criterion is met, then under some sufficiently short forward iteration the distance between two points $\mathbf{p}(i)$ and $\mathbf{p}(j)$ of the reconstructed attractor, which are initially only a small ϵ apart, cannot grow further as $R_{tr}\epsilon$, where R_{tr} is a given constant (see below). However, if an i-th point has a close neighbor that does not fulfill this criterion, then this i-th point is marked as having a false nearest neighbor. We have to minimize the fraction of points having a false nearest neighbor by choosing a sufficiently large embedding dimension m. If m is too small, two points of the attractor may solely appear to be close, whereas under forward iteration they are be mapped randomly due to projection effects. In order to calculate the fraction of false nearest neighbors the following algorithm is used. Given a point $\mathbf{p}(i)$ in the m-dimensional embedding space, one first has to find a neighbor $\mathbf{p}(j)$, so that $\|\mathbf{p}(i)-\mathbf{p}(j)\| \leq \epsilon$, where $\|\ldots\|$ is the square norm and ϵ is a small constant usually not larger than the standard deviation of data. We then calculate the normalized distance R_i between the $(m+1)$-st embedding coordinate of points $\mathbf{p}(i)$ and $\mathbf{p}(j)$

according to the equation:

$$R_i = \frac{|x_{i+m\tau} - x_{j+m\tau}|}{\|\mathbf{p}(i) - \mathbf{p}(j)\|}. \quad (4)$$

If R_i is larger than a given threshold R_{tr}, then $\mathbf{p}(i)$ is marked as having a false nearest neighbor. Equation 4 has to be applied for the whole time series and for various $m = 1, 2, \ldots$ until the fraction of points for which $R_i > R_{tr}$ is negligible. According to Kennel *et al.* [20], $R_{tr} = 10$ has proven to be a good choice for most data sets. Results of the method for the temporal trace in Fig. 1(e) are presented in Fig. 2. It can be observed that the fraction of false nearest neighbors (fnn) drops to zero convincingly at $m = 5$.

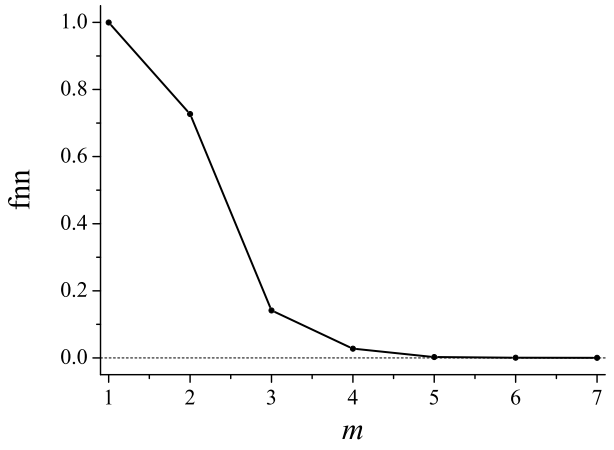

FIG. 2. Calculation of the appropriate embedding dimension m for the waveform presented in Fig. 1(e). The fraction of false nearest neighbors (fnn) drops convincingly to zero at $m = 5$.

We now have all at hand to calculate the maximal Lyapunov exponent Λ_{max} of the studied waveform. We use quite an elaborate algorithm developed by Wolf *et al.* [21] that implements the theory in a very direct fashion. For each point of the embedding space $\mathbf{p}(i)$ find a near neighbor $\mathbf{p}(j)$, which satisfies the relation $\|\mathbf{p}(i)-\mathbf{p}(j)\| \leq \epsilon$. Then iterate both points forward in time for a fixed evolution time ν, which should be similar to the embedding delay τ, but not much larger than $m\tau$. If the system is chaotic, the distance after the evolved time $\|\mathbf{p}(i+\nu)-\mathbf{p}(j+\nu)\| = \epsilon_\nu$, will (on average) be larger than the initial ϵ, while in case of regular behavior $\epsilon \approx \epsilon_\nu$. After each evolution ν a so-called replacement step is attempted in which we look for a new point $\mathbf{p}(k)$ in the embedding space, whose distance to the evolved point $\mathbf{p}(i+\nu)$ should be small (ϵ), under the constraint that the angular separation between the vectors constituted by the points $\mathbf{p}(i+\nu)$ & $\mathbf{p}(j+\nu)$ and $\mathbf{p}(i+\nu)$ & $\mathbf{p}(k)$ is small. This procedure is repeated until the initial point of the trajectory reaches the last one. Finally, the maximal Lyapunov exponent can be calculated according to the equation

$$\Lambda_{max} = \frac{1}{n\nu} \sum_{r=1}^{n} \ln \frac{\epsilon_\nu}{\epsilon}, \quad (5)$$

where n is the total number of replacement steps. Depending on the parameters ϵ and ν, the described algorithm yielding Λ_{max} converges nicely to a positive value, thus allegedly supporting our temptation to declare deterministic chaos in the waveform of a plucked guitar chord. We encourage the reader to use programs available from [14, 15] to verify this and convince her/himself of the deceiving clearness of the result.

If the treatment so far appeared consistent and trustworthy our goal has been achieved, since now the reader has a good motivation to continue reading and discover the lesson to be learned. Of course, much of the above-presented theory will be used also in what follows so that the effort invested so far will not go to waste.

First, it is necessary to diminish the trustworthiness of so-far presented results, in particular by lending support to the fact that linear dynamics alone may also yield such complex waveforms as presented in Fig. 1(e), and thus may not necessarily represent chaotic behavior. For this purpose, it is most elegant to turn to previously published literature relating to the (non)linearity in vibrating strings [13, 22–27]. According to these studies, possible nonlinear effects in freely vibrating strings include an increase in resonant frequency upon increasing the amplitude, skewed resonance curves that reflect such effects, the generation of higher

harmonics [24], a transition from planar to elliptically polarized transverse waves when driven above a given threshold limit [22], and the precession of such elliptical orbits when the string is vibrating freely [24, 25]. However, as pointed out already in those papers, such effects are only significant at very large amplitudes and are generally far too small to be inferred by strings at normal tensions on stringed instruments like the violin, cello or guitar [24], although at certain conditions or a periodic external driving a vibrating string may very well exhibit chaotic behavior [28, 29]. Thus, in order for our study to conform to previous findings, it appears absolutely necessary to conduct further research and elaborate on the behavior presented in Fig. 1(e).

Since the level of sophistication in the above-applied method for determining the maximal Lyapunov exponent is quite high, and apparently leading to essentially wrong results, it appears reasonable to implement less elaborate methods. An obvious and familiar candidate is the Fourier transform [10]. However, since the waveform of the guitar chord evidently incorporates several harmonic and inharmonic frequencies the resulting spectrum has, besides quite well-defined peaks at best expressed frequencies, also a continuous component, which overall results in a transform that remarkably resembles the ones obtained when analyzing so-called intermittent chaotic regimes [10]. Thus, without the information given in the preceding paragraph, it would be difficult to make a definite assessment of the behavior solely on the basis of the Fourier transform (and even more so in view of the maximal Lyapunov exponent obtained via the algorithm of Wolf *et al.* [21]).

As the definite remedy, we propose to use the simple and appealing graphical method of recurrence plots [30]. Recurrent behavior is an inherent property of periodic and to some extend also chaotic systems. In particular, by periodic behavior time-distinct states in the phase space can be arbitrarily close, *i.e.* $\|\mathbf{p}(i) - \mathbf{p}(j)\| = 0$ if times i and j differ exactly by some integer of the oscillation period T, whereas for chaotic systems

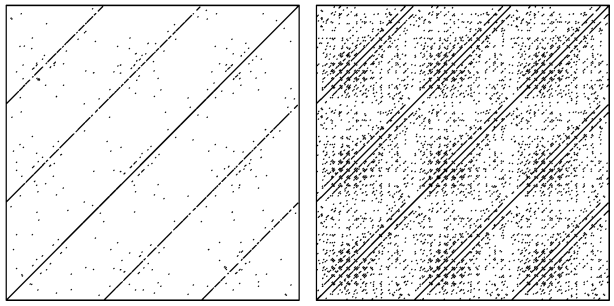

FIG. 3. Recurrence plot analysis of the phase space presented in Fig. 1(e) (reconstructed with $\tau = 70$ and $m = 5$) for $\epsilon = 0.01$ (left) and $\epsilon = 0.03$ (right). See also the main text for details.

this distance is always finite. The recurrence plot is a 2D square-grid graph with time units on both axes, whereby, in the most common case, points (i, j) that satisfy

$$\|\mathbf{p}(i) - \mathbf{p}(j)\| < \epsilon, \tag{6}$$

where $\|\dots\|$ is the square norm and ϵ is a small constant determining the maximally allowed distance between points in the reconstructed phase space, are marked with black dots whilst all others are left white. Remarkably, note that the very same procedure is an integral part of the false nearest neighbor method as well as the algorithm for determining Λ_{max}. Depending on the application, there also exist many variations of recurrence plots [31, 32], but presently the above-outlined basic implementation will totally suffice. In accordance with Eq. 6, it is evident that each recurrence plot (no matter what the input and the value of ϵ) will have a diagonal line along the middle of the graph where $i = j$, since then the condition given by Eq. 6 is trivially satisfied. Following this reasoning, if one examines periodic behavior the satisfaction of the condition $i = j+T$ (and equivalently $j = i + T$), where T is the oscillation period (in dimensionless units) of the examined behavior, will yield additional diagonal lines above and below the central diagonal line starting at each multiple of T. Importantly, if the behavior is truly periodic, all such diagonal lines will be mostly (apart from minute interceptions that might occur due to measurement error) unbroken throughout the recurrence plot, and

moreover, the position of the main diagonal lines will not change when varying ϵ. On the other hand, by chaotic behavior one can still observe diagonal lines above and bellow the central diagonal, but these are heavily scattered, interrupted by isolated points, and perhaps most importantly, do not occur every multiple of T due to the lack of a precisely defined oscillation period, but appear randomly throughout the recurrence plot. Also, the outlay of a recurrence plot of chaotic data will typically change when varying ϵ. To see examples of recurrence plots obtained for chaotic data sets please visit the Web page of Norbert Marwan [32] where a large collection is maintained and easily accessible. Presently, we focus on the waveform of the studied guitar chord presented in Fig. 1(e). The recurrence plots presented in Fig. 3 can be obtained with the program *recurrplot.exe* [14] where the main input parameters are the previously determined embedding delay $\tau = 70$, embedding dimension $m = 5$, and the value of ϵ. It is evident that irrespective of ϵ the main diagonal lines, occurring at each multiple of T (note that the lines are equally separated), are largely unbroken and their position remains unchanged. Of course, one has to keep in mind the fact that we are still analyzing real life recordings, which are always somewhat burdened by measurement error, and also the amplitude of the plucked strings decays minutely during the time span of the studied recording; thus $\|\mathbf{p}(i) - \mathbf{p}(i+T)\| = 0$ is unattainable. However, the value of $\epsilon = 0.01$ used for the left panel of Fig. 3 represents only 1/100 of the total interval spanned by the time series (note that we have, for simplicity and easier comparisons, rescaled all series to the unit interval), and thus indicates that the temporal activity is repetitious within a minute error margin that is far lower than can be expected for chaotic systems. If ϵ is increased the revealed main periodicity remains unchanged, but also additional temporal correlations can be identified. In sum, results presented in Fig. 3 give ample evidence that the waveform of the studied guitar chord is indeed periodic, and as emphasized already in previous works [24], is produced virtually exclusively by the linear dynamics behind the mechanics of freely vibrating strings at normal tensions on stringed instruments like the violin, cello or guitar. As such, the observed complexity of the studied waveform is simply a consequence of the superposition of the harmonic and inharmonic frequencies emitted by each string and the body of the instrument, which is, however, a purely linear phenomenon and thus in accordance with the theory of nonlinear dynamical systems [1–4] strictly unable to produce chaotic behavior.

3. Summary

We analyze waveforms of increasingly complex sounds with methods of time series analysis, showing that the transition from monotonous humming produced by a frequency generator towards the sound of a guitar chord is, despite the apparent emergence of irregular chaotic behavior, adequately described by linear dynamics alone, as such yielding periodic temporal traces. Importantly, the obtained wrong positive maximal Lyapunov exponent indeed appears to be a consequence of the sophistication behind the algorithm for calculating it, rather than the complexity incorporated in the studied time series. Although the possibility of such pitfalls is often mentioned in books [9–11], explicit examples are rarely given. Remarkably, the cure against such spurious results can be found basically by implementing a small part of the algorithm for calculating Λ_{max} (at least in the present case, but most likely the approach will work beautifully elsewhere as well) in the form of a recurrence plot, thus impressively demonstrating that it is always wise to first implement simple algorithms yielding clearly interpretable and traceable results before attempting additional more sophisticated investigations.

It is our hope that the study will find its place also in graduate courses as an interesting example of how observed complex behavior, consisting of dozens of harmonic and inharmonic frequencies, may not necessarily imply chaos, and

moreover, how conceptually simple methods may often yield better results in comparison to their more elaborate counterparts. Finally, we would like to note that methods of time series analysis could be successfully applied also to other sounds, such as human vocals or those produced by wind instruments, thus providing a vast playground enabling students to familiarize themselves with basic features as well as pitfalls of the methods.

Acknowledgement

Matjaž Perc is thankful for the support from the Slovenian Research Agency (grant Z1-2032-2547).

References

[1] H. G. Schuster, *Deterministic chaos* (VCH, Weinheim, 1989).
[2] S. H. Strogatz, *Nonlinear dynamics and chaos* (Addison-Wesley, Massachusetts, 1994).
[3] R. C. Hilborn, *Chaos and nonlinear dynamics* (Oxford University Press, Oxford, 1994).
[4] D. T. Kaplan and L. Glass, *Understanding nonlinear dynamics* (Springer, New York, 1995).
[5] K. Briggs, Am. J. Phys. **55**, 1083 (1987).
[6] N. B. Tufillaro, T. A. Abbott, and J. P. Reilly, *An experimental approach to nonlinear dynamics and chaos* (Addison-Wesley, Massachusetts, 1992).
[7] T. Timberlake, Am. J. Phys. **72**, 1002 (2004).
[8] L. E. Matson, Am. J. Phys. **75**, 1114 (2007).
[9] H. D. I. Abarbanel, *Analysis of observed chaotic data* (Springer, New York, 1996).
[10] H. Kantz and T. Schreiber, *Nonlinear time series analysis* (Cambridge University Press, Cambridge, 1997).
[11] J. C. Sprott, *Chaos and time-series analysis* (Oxford University Press, Oxford, 2003).
[12] We note that the modes of a plucked guitar string are not exactly higher harmonics of the ground frequency because of the finite rigidity of the string, and because the bridge support transmitting energy to the body of the instrument is not a perfect node. However, these effects are currently not of vital importance, but will be addressed briefly in the next section.
[13] C. Vallette, in *Mechanics of musical instruments* edited by A. Hirschberg, J. Kergomard, and G. Weinreich (Springer, New York, 1995), p. 115.
[14] Results presented in this paper can be reproduced with programs that can be downloaded from the Web page (Matjaž Perc) `http://www.matjazperc.com/ejp/time.html`
[15] The official Web page of the TISEAN project is `http://www.mpipks-dresden.mpg.de/~tisean/`
[16] R. Hegger and H. Kantz, Chaos **9**, 413 (1999).
[17] T. Sauer, J. A. Yorke, and M. Casdagli, J. Stat. Phys. **65**, 579 (1991).
[18] R. Shaw, Z. Naturforsch. **36a**, 80 (1981).
[19] A. M. Fraser and H. L. Swinney, Phys. Rev. A **33**, 1134 (1986).
[20] M. B. Kennel, R. Brown, and H. D. I. Abarbanel, Phys. Rev. A **45**, 3403 (1992).
[21] A. Wolf, J. B. Swift, H. L. Swinney, and J. A. Vastano, Physica D **16**, 285 (1985).
[22] J. A. Elliot, Am. J. Phys. **48**, 478 (1980).
[23] K. Legge and N. H. Fletcher, J. Acoust. Soc. Am. **76**, 5 (1984).
[24] C. E. Gough, J. Acoust. Soc. Am. **75**, 1770 (1984).
[25] J. Miles, J. Acoust. Soc. Am. **75**, 1505 (1984).
[26] R. J. Hanson, J. M. Anderson, and H. K. Macomber, J. Acoust. Soc. Am. **96**, 1549 (1994).
[27] R. J. Hanson, H. K. Macomber, A. C. Morrison, and M. A. Boucher, J. Acoust. Soc. Am. **117**, 400 (2005).
[28] N. B. Tufillaro, Am. J. Phys. **57**, 408 (1989).
[29] T. C. Molteno and N. B. Tufillaro, Am. J. Phys. **72**, 1157 (2004).
[30] J.-P. Eckmann, S. O. Kamphorst, and D. Ruelle, Europhys. Lett. **5**, 973 (1987).
[31] N. Marwan, *Encounters with neighbours - Current developments of concepts based on recurrence plots and their applications* (PhD Thesis, University of Potsdam, 2003).
[32] Recurrence plot Web page of Norbert Marwan is `http://www.recurrence-plot.tk/`